Title: Propagation of THz irradiation energy through aqueous layers: Demolition of actin filaments in living cells

Authors:
Shota Yamazaki,[1*] Masahiko Harata,[2] Yuya Ueno,[2] Masaaki Tsubouchi,[3] Keiji Konagaya,[4] Yuichi Ogawa,[4] Goro Isoyama,[5] Chiko Otani[1] and Hiromichi Hoshina[1*]

Affiliations:
[1]RIKEN, Center for Advanced Photonics, 519-1399 Aramaki-Aoba, Aoba-ku, Sendai, Miyagi, 980-0845 Japan.
[2]Laboratory of Molecular Biology, Graduate School of Agricultural Science, Tohoku University, Sendai, Japan.
[3]Kansai Photon Science Institute, National Institutes for Quantum and Radiological Science and Technology, Kyoto 619-0215, Japan.
[4]Department of Physics, Graduate School of Science, Kyoto University, Kitashirakawa-oiwakecho, Sakyo-ku, Kyoto 606-8502, Japan.
[5]Institute of Scientific and Industrial Research, Osaka University, 8-1 Mihogaoka, Ibaraki, Osaka, 567-0047, Japan.
*Correspondence and requests for materials should be addressed to S.Y. (email: shota.yamazaki.fc@riken.jp) or H.H. (hoshina@riken.jp)

Abstract: The effect of terahertz (THz) radiation on deep tissues of human body has been considered negligible due to strong absorption by water molecules. However, we observed that the energy of THz pulses transmits a millimeter thick in the aqueous solution, possibly as a shockwave, and demolishes actin filaments. Collapse of actin filament induced by THz irradiation was also observed in the living cells under an aqueous medium. We also confirmed that the viability of the cell was not affected under the exposure of THz pulses. The potential of THz waves as an invasive method to alter protein structure in the living cells is demonstrated.

One sentence summary:
The energy of the THz wave propagates several millimeters into an aqueous medium and demolishes actin filaments via shockwaves.

MAIN TEXT

Due to the development of terahertz (THz) light sources, various and medical applications have been proposed in this decades. Also, toxicity of THz radiation for human health has attracted keen interest among researchers working in this frequency region (*1*). Two projects, the European THz-BRIDGE and the International EMF project in the SCENIHR (*2*), summarize recent studies about THz radiation effects for human body. For example, non-thermal impacts on DNA stability (*3–5*) was induced by THz wave, which could cause chromosomal aberrations in human lymphocytes (*6*). The transcriptional activation of wound-responsive genes in mouse skin (*7*) and DNA damage in an artificial human 3D skin tissue model (*8*) have also been demonstrated. Most of those studies focus on epithelial and corneal cell lines, because THz photons are totally absorbed at the surface of the tissues due to the intense absorbance of liquid water in this frequency region.

However, if the THz radiation is converted to the other type of energy flow which can propagate into water, irradiation of THz wave may cause damage inside the tissues. In fact, the THz photon energy is once absorbed on the body surface, and converted to the thermal and mechanical energies. We recently observed that THz pulses generate shockwaves at the surface of liquid water (*9*). The

generated shockwaves propagate several millimeters in depth. Similar phenomena may occur at the human body. The THz-induced shockwaves may induce mechanical stress to the biomolecules and change their morphology. Such indirect effects of the THz irradiation have not been investigated.

To reveal the effect of THz-induced shockwaves to the biological molecules, we focused on morphology of the actin proteins. Actin has two functional forms, monomeric globular (G)-actin and polymerized filamentous (F)-actin. The actin filament forms the elaborate cytoskeleton network, which plays crucial roles in cell shape, motility, and division (*10*). One advantage of using actin is that we can easily obtain enough purified G-actin from tissues (*11*) to reconstruct polymerization reactions *in vitro*. Actin filaments can be directly observed by fluorescence microscopy by staining with silicon-rhodamine (SiR)-actin (*12*). In this study, we investigated the effect of THz-induced shockwaves on actin filaments. The experiments were performed by the actin aqueous solution and living cell with several THz wave energy densities and shockwave propagation lengths. We also confirmed that the viability of the cell was not affected under the exposure of THz pulses. The potential of THz waves as an invasive method to alter protein structure in the living cells is demonstrated.

To mimic the effect of THz irradiation on tissue proteins, a 1 mm-thick aqueous solution of actin protein was subjected to THz pulsed irradiation (Fig. 1A). During actin polymerization, 80 μJ/cm^2/micro-pulse THz pulses were applied from the bottom of the dish. After 30-min THz irradiation, a portion of the actin solution was collected for fluorescence microscope observation. The irradiated sample (Fig. 1B, right) clearly lost brightness as compared to the control (Fig. 1B, left), and the number of actin filaments with detectable length decreased. The number of actin filaments was decreased about 50% by the THz pulses (Fig. 1C). Figure 1D shows examples of the magnified images of actin filaments. Actin filaments formed straight structures, and morphological deformation such as branching or molecular aggregation was not observed. Therefore, we conclude that THz irradiation decreases actin filaments, but does not denature actin molecules.

Since the reaction rate is temperature-dependent, reduced actin filaments could be explained by increased temperature of water due to absorption of THz waves (Fig. S1A). Using an adiabatic model, temperature was increased at the solution surface by about 0.035 °C with a single micro-pulse (Fig. S1B). The solution surface was then cooled by thermal diffusion in the interval between pulses. Thus, the average temperature gradually increases during irradiation of THz pulses until reaching equilibrium. Sample temperature measured at the end of irradiation was 1.4 °C higher than the control. However, actin polymerization does not show remarkable changes until 50 °C (*13*, *14*). Increasing the temperature by a few °C does not explain the inhibition of polymerization reaction. Another mechanism must be considered.

When intense, ultrashort laser pulses are focused on a biological material, various nonlinear photophysical and photochemical processes are induced. We recently observed that THz pulses effectively generate shockwaves, which propagates a few millimeters into the aqueous medium (*9*). Therefore, shockwave propagation is the most likely reason for THz-induced decrease in actin filaments. To demonstrate the THz pulse radiation effect deeper into the aqueous layer, we observed morphological changes in actin fibrils from living cells. The cells were sunk in the culture medium to avoid direct interaction with the THz wave and rapid temperature change. HeLa cells were grown on a glass plate and placed 800 μm away from the bottom of the dish to simulate similar depth from a tissue surface. The culture medium was kept at 37 °C during the experiment and THz pulses were applied from the bottom of the dish (Fig. S2).

In HeLa cells, actin filaments form several assemblies categorized as cell cortex fibers, stress fibers, and cytoplasmic actin filaments, which are present in different cellular regions. To observe morphological changes, endogenous actin filaments were observed with a fluorescent microscope. HeLa cells were stained with SiR-actin for live-cell imaging before (Fig. 2A, i-iv) and after 30-minute THz irradiation (Fig. 2A, v-viii). The energy of the THz micro-pulse was 0, 80, 160, 250 μJ/cm^2, respectively. Intact actin filament structure is clearly observed at before THz irradiation in all samples (Fig. 2A, i-iv). This structure was maintained after 30 minutes in control cells (Fig. 2A, v), showing that no significant damage occurs from the UV light of the microscope. After THz irradiation, actin filaments were decreased and actin aggregates were observed in the cell cortex (Fig. 2A, vi-viii, red arrow), which is a layer of thin actin filaments formed at the cell periphery and plays important roles in cell morphology, migration, and invasion.

To observe detailed actin filament structure within the cell cortex, cells were immunostained with AlexaFluor 594 Phalloidin and observed by spinning-disk confocal microscopy after THz irradiation for 30 minutes (Fig. 2B, i-iv and v-viii (zoomed images)). The samples after 80 and 160 μJ/cm^2 THz irradiation show a dark area in the cell cortex (Fig. 2B, vi and vii), indicating disassembly of the actin filaments. Actin aggregation is present near the cell periphery (Fig. 2B, iv and viii, red allow) after 250 μJ/cm^2 irradiation. We also observed severed filopodia in these cells (Fig. 2B, iv, red allow head). Artificial collapse of actin filaments with chemical reagents causes aggregation of actin filaments (*15*), which is similar to the phenomenon shown in Fig. 2B, iv. These results demonstrate that actin filaments are disrupted with high THz irradiation power.

To examine the energy transport in water induced by THz irradiation, we observed morphological changes in actin fibrils at various distances from the irradiating point (Fig. 3). Cells were positioned 800, 1800, and 2800 μm away from the interface. Similar to Fig. 2, cells were imaged before and after THz irradiation with 250 μJ/cm^2 micro-pulse energy (Fig. 3A). Figure 3B shows high-resolution images of the cell cortex after irradiation for 30 minutes. Note that the images at 800 μm and control are taken from Fig. 2 for comparison. The live-cell images at 1800 μm show that the actin filaments disappeared and actin aggregated (Fig. 3A, vii), similar to images at 800 μm (Fig. 3A, vi), which is also present in the high-resolution images (Fig. 3B, vii, red arrow). However, aggregate size is smaller than at 800 μm. At 2800 μm, actin aggregation is not clearly observed (Fig. 3A, viii) and large peripheral actin filaments remain after irradiation (Fig. 3B, viii). This result demonstrates that the energy of the THz wave propagates more than 1000 μm into an aqueous solution, which means that the irradiated photon energy is converted to another type of traveling energy, i.e. thermal or pressure energy. The temperature change due to the THz irradiation is negligibly small in these experimental conditions. Therefore, the irradiated THz photon energy propagates as a shockwave, which demolishes cellular actin filaments in culture. This result corroborates previous reports which observed that shockwaves generated by piezoceramic vibrator induces actin filament fragmentation (*16*, *17*). The shockwaves with 16 MPa peak pressure are focused on culture cell and destroys the cell cortex and filopodia, similar to our results (Figs. 2 and 3).

Shockwaves are used for medical and biological applications, such as surgery, gene therapy, and drug delivery. In general, the laser-induced shockwaves are generated by focused light. The energy of the high-power laser pulses is converted to shockwaves by the formation of plasma and cavitation bubbles. However, such high-energy phenomena cause the loss of peripheral cells and serious cellular damage (*16*–*19*). On the other hand, THz energy is effectively transferred to the mechanical energy of the shockwave with nondestructive processes. To confirm the “softness” of

shockwave generation via THz irradiation, cell death was measured by a cytotoxicity assay using 4',6-diamidino-2-phenylindole (DAPI). When cell death or loss of membrane integrity occurs, DAPI is taken into the cytoplasm through the damaged membrane and generates fluorescence after DNA binding. Figure 4A shows cells before and after THz irradiation with 250 $\mu J/cm^2$. Cell shape was maintained after 30-min exposure. Figure 4B shows fluorescence images of DAPI. Figure 4C shows merged image between visible cells and DAPI fluorescence. Less than 1% of cells show fluorescence after THz irradiation, similar to control experiments. These results indicate that membrane injury or cell death is not induced by THz irradiation, but that manipulation of actin filaments in living cells might be induced by THz waves as shown in Figs. 2 and 3.

In summary, we demonstrate that THz pulses change actin filament morphology in aqueous solutions via shockwaves. THz irradiation affects not only the surface of the human body, but also a few millimeters into the tissue. This penetration should be considered when developing high-power THz radiation safety standards. These results also indicate that THz irradiation could be applicable for nondestructive manipulation of cellular functions by modulation of actin filaments.

References and Notes:

1. H. Hintzsche, H. Stopper, Effects of terahertz radiation on biological systems. *Crit. Rev. Environ. Sci. Technol.* **42**, 2408–2434 (2012).
2. N. Leitgeb, A. Auvinen, H. Danker-hopfe, K. H. Mild, *SCENIHR (Scientific Committee on Emerging and Newly Identified Health Risks), Potential health effects of exposure to electromagnetic fields (EMF), Scientific Committee on Emerging and Newly Identified Health Risks SCENIHR Opinion on Potential health* (2016).
3. J. Bock, Y. Fukuyo, S. Kang, M. Lisa Phipps, L. B. Alexandrov, K. O. Rasmussen, A. R. Bishop, E. D. Rosen, J. S. Martinez, H. T. Chen, G. Rodriguez, B. S. Alexandrov, A. Usheva, Mammalian stem cells reprogramming in response to terahertz radiation. *PLoS One*. **5**, 8–13 (2010).
4. B. S. Alexandrov, K. Ø. Rasmussen, A. R. Bishop, A. Usheva, L. B. Alexandrov, S. Chong, Y. Dagon, L. G. Booshehri, C. H. Mielke, M. L. Phipps, J. S. Martinez, H.-T. Chen, G. Rodriguez, Non-thermal effects of terahertz radiation on gene expression in mouse stem cells. *Biomed. Opt. Express*. **2**, 2679 (2011).
5. B. S. Alexandrov, M. Lisa Phipps, L. B. Alexandrov, L. G. Booshehri, A. Erat, J. Zabolotny, C. H. Mielke, H. T. Chen, G. Rodriguez, K. O. Rasmussen, J. S. Martinez, A. R. Bishop, A. Usheva, Specificity and Heterogeneity of Terahertz Radiation Effect on Gene Expression in Mouse Mesenchymal Stem Cells. *Sci. Rep.* **3**, 1–8 (2013).
6. A. Korenstein-Ilan, A. Barbul, P. Hasin, A. Eliran, A. Gover, R. Korenstein, Terahertz Radiation Increases Genomic Instability in Human Lymphocytes. *Radiat. Res.* **170**, 224–234 (2008).
7. K. T. Kim, J. Park, S. J. Jo, S. Jung, O. S. Kwon, G. P. Gallerano, W. Y. Park, G. S. Park, High-power femtosecond-terahertz pulse induces a wound response in mouse skin. *Sci. Rep.* **3**, 1–7 (2013).
8. L. V. Titova, A. K. Ayesheshim, A. Golubov, D. Fogen, R. Rodriguez-Juarez, F. A. Hegmann, O. Kovalchuk, Intense THz pulses cause H2AX phosphorylation and activate DNA damage response in human skin tissue. *Biomed. Opt. Express*. **4**, 559 (2013).
9. M. Tsubouchi, H. Hoshina, M. Nagai, G. Isoyama, Plane shockwave generation in liquid water using irradiation of terahertz pulses. *arXiv* (2019) (available at http://arxiv.org/abs/1911.04674).

10. J. V Small, K. Rottner, I. Kaverina, K. I. Anderson, Assembling an actin cytoskeleton for cell attachment and movement. *Biochim. Biophys. Acta*. **1404**, 271–281 (1998).
11. J. A. Cooper, S. B. Walker, T. D. Pollard, Pyrene actin: documentation of the validity of a sensitive assay for actin polymerization. *J. Muscle Res. Cell Motil.* **4**, 253–262 (1983).
12. E. D'Este, S. W. Hell, H. Waldmann, F. Göttfert, D. W. Gerlich, A. Masharina, A. Güther, H. Ta, S. Rizzo, C. Blaukopf, G. Lukinavičius, C. Sommer, M. Fournier, L. Reymond, H.-D. Arndt, K. Johnsson, Fluorogenic probes for live-cell imaging of the cytoskeleton. *Nat. Methods*. **11**, 731–733 (2014).
13. S. Yamazaki, M. Harata, T. Idehara, K. Konagaya, G. Yokoyama, H. Hoshina, Y. Ogawa, Actin polymerization is activated by terahertz irradiation. *Sci. Rep.* **8** (2018), doi:10.1038/s41598-018-28245-9.
14. M. KAWAMURA, K. MARUYAMA, A Further Study of Electron Microscopic Particle Length of F-Actin Polymerized *in Vitro*. *J. Biochem.* **72**, 179–188 (1972).
15. T. Wakatsuki, B. Schwab, N. C. Thompson, E. L. Elson, Effects of cytochalasin D and latrunculin B on mechanical properties of cells. *J. Cell Sci.* **114**, 1025–1036 (2001).
16. P. Steinbach, F. Hofstadter, H. Nicolai, W. Rossler, W. Wieland, In vitro investigations on cellular damage induced by high energy shock waves. *Ultrasound Med. Biol.* **18**, 691–699 (1992).
17. S. F. Moosavi-Nejad, S. H. R. Hosseini, M. Satoh, K. Takayama, Shock wave induced cytoskeletal and morphological deformations in a human renal carcinoma cell line. *Cancer Sci.* **97**, 296–304 (2006).
18. C.-D. Ohl, B. Wolfrum, Detachment and sonoporation of adherent HeLa-cells by shock wave-induced cavitation. *Biochim. Biophys. Acta*. **1624**, 131–138 (2003).
19. T. BrÄuner, F. Brümmer, D. F. Hülser, Histopathology of shock wave treated tumor cell suspensions and multicell tumor spheroids. *Ultrasound Med. Biol.* **15**, 451–460 (1989).
20. K. Kawase, R. Kato, A. Irizawa, M. Fujimoto, S. Kashiwagi, Nuclear Instruments and Methods in Physics Research A The high-power operation of a terahertz free-electron laser based on a normal conducting RF linac using beam conditioning. *Nucl. Inst. Methods Phys. Res. A.* **726**, 96–103 (2013).
21. S. Suemine, K. Kawase, N. Sugimoto, S. Kashiwagi, K. Furukawa, R. Kato, A. Irizawa, M. Fujimoto, H. Ohsumi, M. Yaguchi, S. Funakoshi, R. Tsutsumi, K. Kubo, A. Tokuchi, G. Isoyama, Nuclear Instruments and Methods in Physics Research A Grid pulser for an electron gun with a thermionic cathode for the high-power operation of a terahertz free-electron laser. *Nucl. Inst. Methods Phys. Res. A.* **773**, 97–103 (2015).
22. H. R. Zelsmann, M. Condensie, S. Moticulatre, Temperature dependence of the optical constants for liquid H2O and D2O in the far IR region. *J. Mol. Struct.* **350**, 95–114 (1995).
23. G. S. Settles, *Schlieren and shadowgraph techniques: visualizing phenomena in transparent media* (Springer Science & Business Media, 2012).
24. M. Greenspan, C. E. Tschiegg, Tables of the speed of sound in water. *J. Acoust. Soc. Am.* **31**, 75–76 (1959).
25. P. H. Rogers, Weak-shock solution for underwater explosive shock waves. *J. Acoust. Soc. Am.* **62**, 1412–1419 (1977).
26. B. D. Strycker, M. M. Springer, A. J. Traverso, A. A. Kolomenskii, G. W. Kattawar, A. V Sokolov, Femtosecond-laser-induced shockwaves in water generated at an air-water interface. *Opt. Express*. **21**, 23772–23784 (2013).
27. M. F. Hamilton, D. T. Blackstock, *Nonlinear acoustics* (Academic press San Diego,

1998), vol. 237.

Acknowledgments:

Funding: This work was supported by Japan Society for the Promotion of Science (JSPS) KAKENHI Grant Numbers JP19K15812 This work was performed under the Cooperative Research Program of "Network Joint Research Center for Materials and Devices." **Author contributions:** S. Y., M. H., Y. O., C. O., and H. H conceived this study. S.Y., Y. U., M.T., and K. K. conducted the experiments and analyzed data. G.I. constructed and managed the THz-FEL facility in Osaka Univ. S.Y., M. T., and H. H. drafted the original manuscript, and all authors edited and reviewed the manuscript. **Competing interests:** The authors declare no competing interests. **Data and materials availability:** The data presented in this manuscript are tabulated in the main paper and in the supplementary materials.

Supplementary Materials:

Material and Methods

Fig. S1-S3

References (*20–27*)

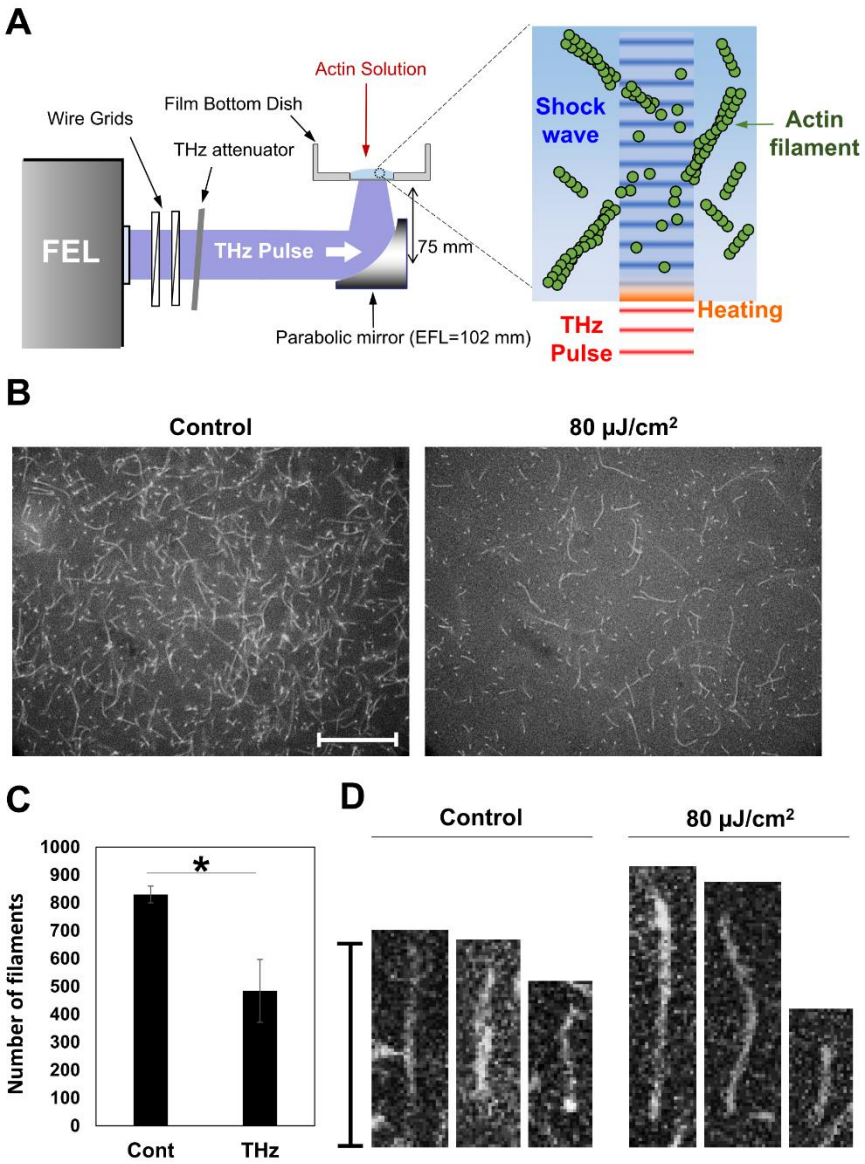

Figure 1. Actin polymerization affected by THz irradiation in an aqueous solution.

(A) Schematic diagram of the experimental set-up. Actin solution was placed in a film bottom dish. THz waves (4 THz) were applied to the bottom of the dish. After THz irradiation, a portion of the actin solution was collected for fluorescence microscope observation. (B) Fluorescence microscopy images of actin filaments with (control, left) or without THz irradiation (80 μJ/cm^2, right). Actin solution (2.4 μM) was fixed and stained with SiR-actin after polymerizing for 30 min. (C) The number of actin filaments counted from fluorescence images. Data shown are the mean and the standard deviation of three independent experiments. More than 300 actin filaments were counted in each of the experiments. Asterisk indicate a statistically significant difference (*P< 0.05). (D) Magnified images of single actin filaments. The bar shows a scale of 20 μm.

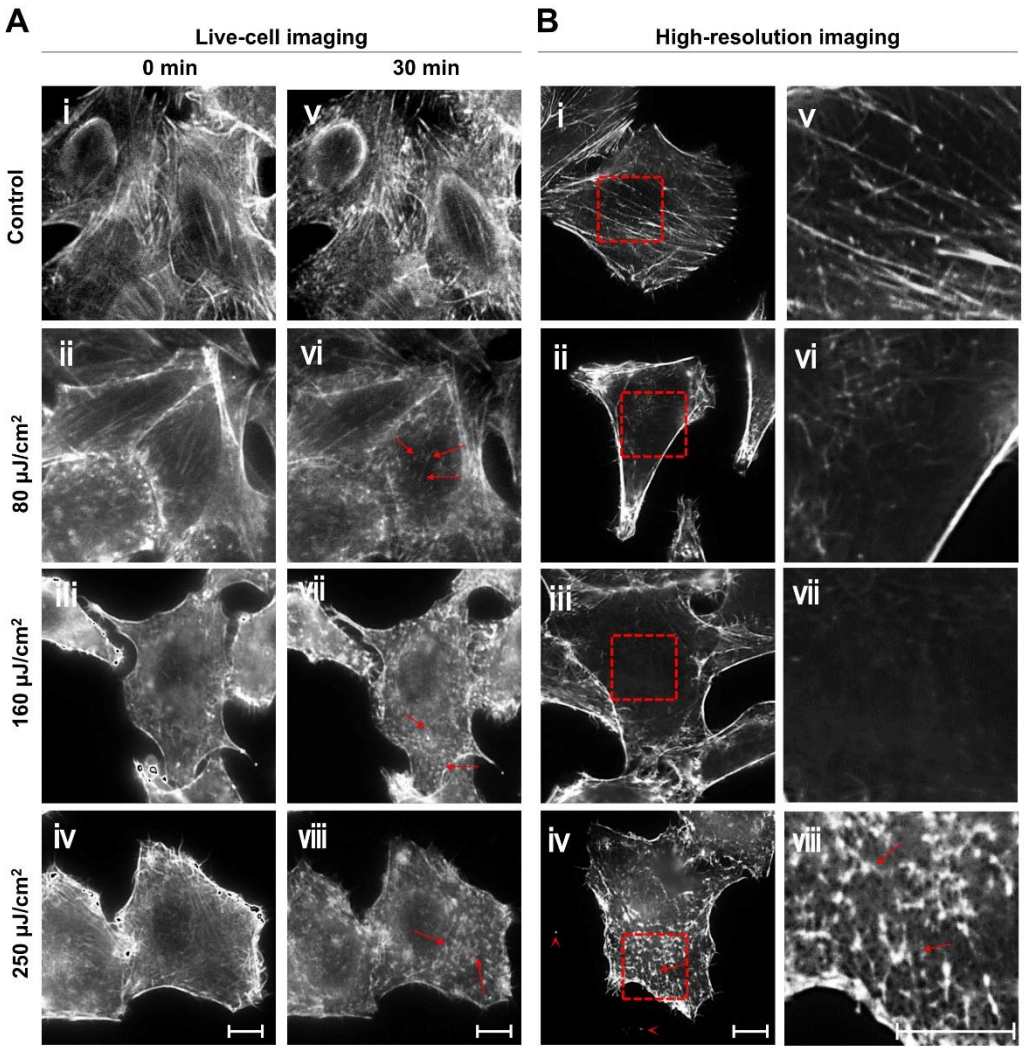

Figure 2. THz wave effects on cellular actin filaments.

(A) Live-cell imaging of actin filaments. The energy of the THz irradiation was 0, 80, 160, and 250 μJ/cm^2. Cells imaged before (A, i-iv) and after 30-minute THz irradiation (A, v-viii). The red arrows indicate aggregated actin filaments. (B) Immunofluorescence images of the cell cortex stained with AlexaFluor 594-phalloidin. Images were observed using spinning-disk confocal microscopy. The right panels (v-viii) show the magnified images of the red squares in the left panels (i-iv), respectively. Red arrows indicate aggregated actin filaments. Arrowheads indicate filipodia fragments. Actin filaments were stained with SiR-actin and observed by fluorescence microscopy. The bar shows a scale of 10 μm.

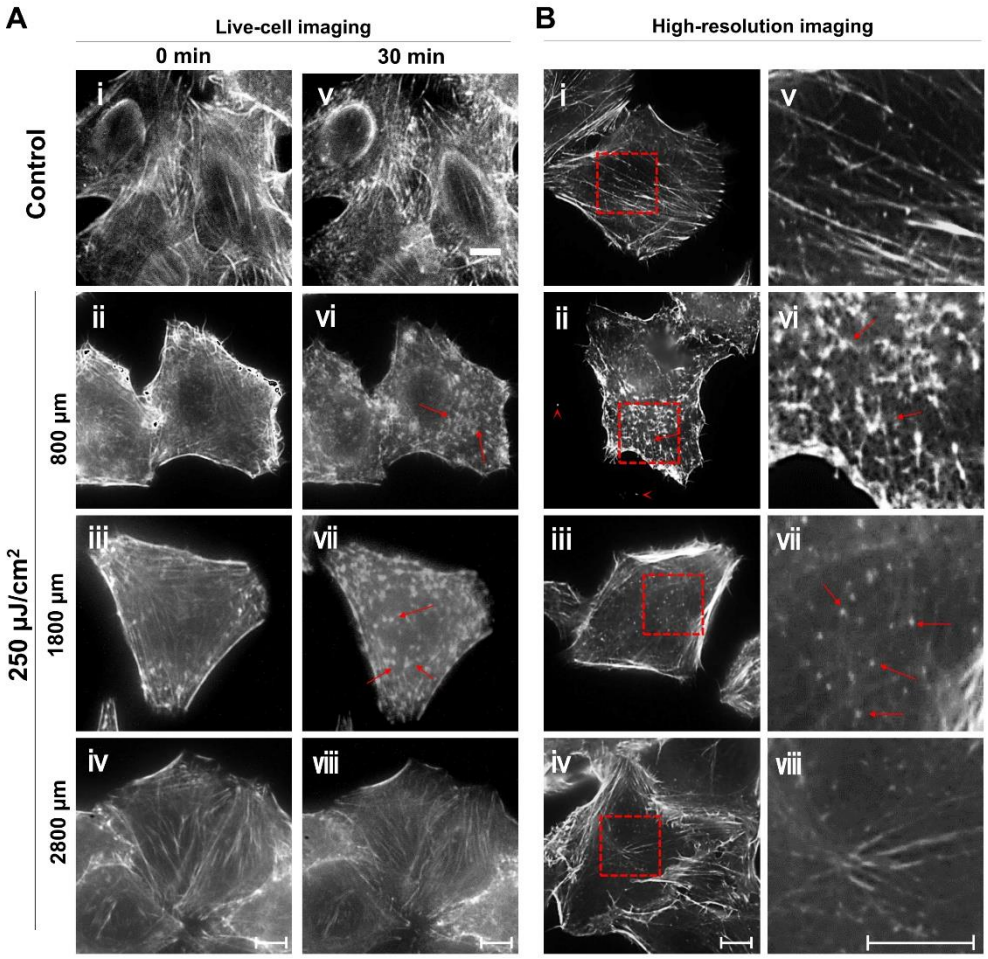

Figure 3. Propagation of THz energy through aqueous culture medium.
(A) Live-cell imaging of actin filaments 800, 1800, and 2800 μm away from the bottom of dish. Control cells were placed 800 μm above the dish bottom. Cells imaged before (A, i-iv) and after (A, v-viii) THz radiation with the energy of 250 μJ/cm^2 for 30 minutes. (B) Immunofluorescence images of the cell cortex stained with AlexaFluor 594-phalloidin. Images were observed using spinning-disk confocal microscopy. The right panels (v-viii) show the magnified images of the red squares in the left panels (i-iv), respectively. Red arrows indicate aggregated actin filaments. Note that the images at 800 μm and control are taken from Fig. 2 for comparison. The bar shows a scale of 10 μm.

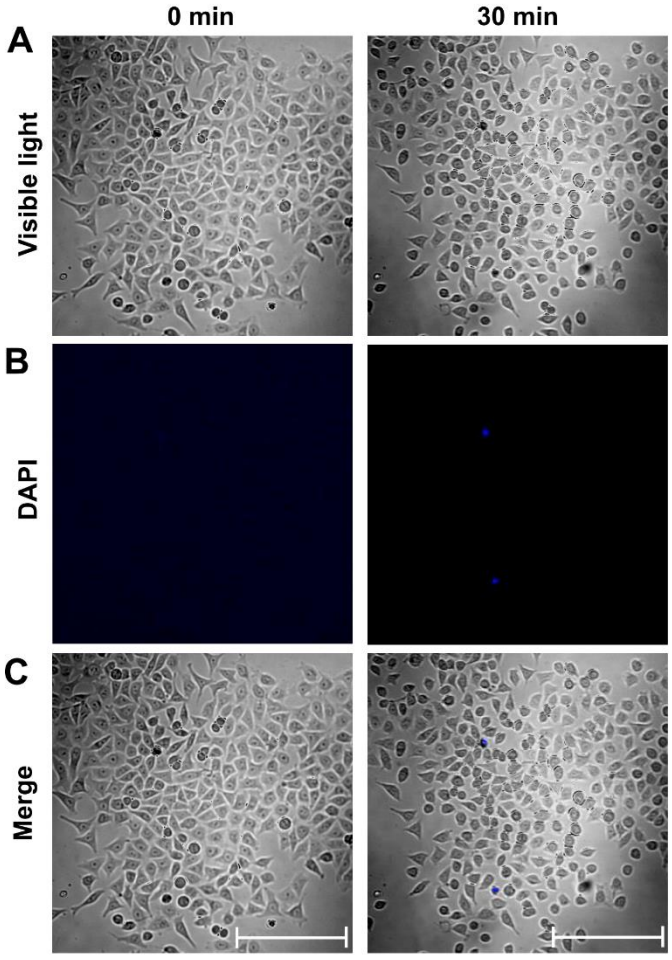

Figure 4. Evidence for no-cytotoxicity by THz irradiation.

(A) Visible images of cells. (B) Fluorescence images of DAPI-stained cells. (C) Merged image of visible cells and DAPI fluorescence. DAPI was added to the culture medium at 0.1 μg/mL to detect cell death. The applied THz wave power density was 250 μJ/cm^2. The cells were placed 800 μm away from the bottom of dish. The bar shows a scale of 100 μm.